Obligatory steps in protein folding and the conformational diversity of the transition state

Jose C. Martinez[1,2], M. Teresa Pisabarro[1] and Luis Serrano[1]

We have analyzed the existence of obligatory steps in the folding reaction of the α-spectrin SH3 domain by mutating Asp 48 (D48G), which is at position *i+3* of an isolated two-residue type II' β–turn. Calorimetry and X-ray analysis show an entropic stabilizing effect resulting from local changes at the dihedral angles of the β-turn. Kinetic analysis of D48G shows that this β-turn is fully formed in the transition state, while there is no evidence of its formation in an isolated fragment. Introduction of several mutations in the D48G protein reveals that the local stabilization has not significantly altered the transition state ensemble. All these results, together with previous analysis of other α-spectrin and src SH3 mutants, indicate that: (i) in the folding reaction there could be obligatory steps which are not necessarily part of the folding nucleus; (ii) transition state ensembles in β-sheet proteins could be quite defined and conformationally restricted ('mechanic folding nucleus'); and (iii) transition state ensembles in some proteins could be evolutionarily conserved.

Our views about how proteins fold have changed dramatically over the past few years. The finding that small monomeric proteins (less than ~100 amino acids) with no disulfide bridges or *cis*-Pro bonds fold in a two-state manner[1–11], has raised questions about the role of early folding intermediates, the nature of the transition state or high energy barrier[12], and the importance of secondary structure elements in protein folding and stability[13]. The 'new view' of protein folding, which has emerged in recent years from a combination of experimental and theoretical approaches, postulates that the folding process could be seen as a parallel flow of an ensemble of chain molecules that follow multiple folding routes to reach the native state[14]. In this scheme the transition state is not considered as a single obligatory step through which all molecules pass, but rather it is an ensemble of many different chain conformations[15]. However, some native contacts will be more probable than others due to the polymeric nature of the chain and the topology of the native state. Analysis of different proteins[16–18] by the protein engineering method[12] indicates that the transition state is consistent with a collapsed globule that crudely resembles the native state, buries a large hydrophobic surface, and has some specific interactions mainly located in the hydrophobic core[17,18]. These results are in agreement with the nucleation-condensation model of protein folding[17,19], in which folding is initiated through a search of conformations until sufficient specific tertiary interactions are made that then act as a scaffold for subsequent contacts[19]. Once this 'nucleus' is built, the protein passes through the transition state, followed by the rapid cooperative formation of the folded structure. The main discrepancy between different folding

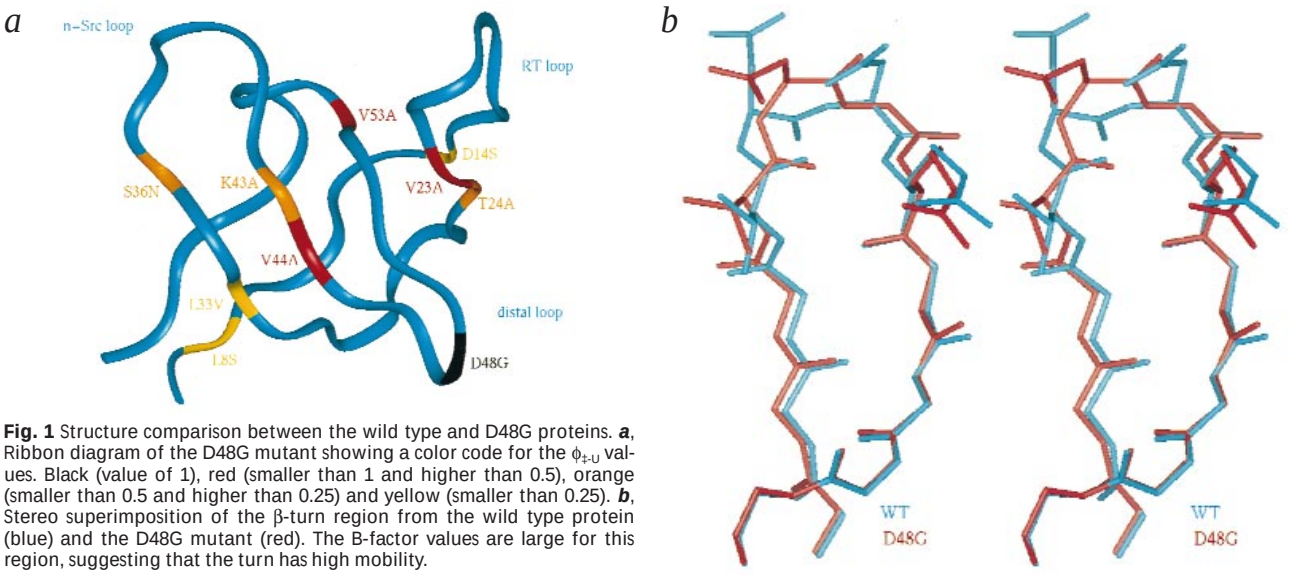

Fig. 1 Structure comparison between the wild type and D48G proteins. ***a***, Ribbon diagram of the D48G mutant showing a color code for the $\phi_{\ddagger-U}$ values. Black (value of 1), red (smaller than 1 and higher than 0.5), orange (smaller than 0.5 and higher than 0.25) and yellow (smaller than 0.25). ***b***, Stereo superimposition of the β-turn region from the wild type protein (blue) and the D48G mutant (red). The B-factor values are large for this region, suggesting that the turn has high mobility.

[1]EMBL, Meyerhofstrasse 1, 69117-Heidelberg, Germany. [2]Departamento de Quimica Fisica, Facultad de Ciencias, Universidad de Granada, 18071-Granada, Spain.

Correspondence should be addressed to L.S. *email: serrano@embl-heidelberg.de*

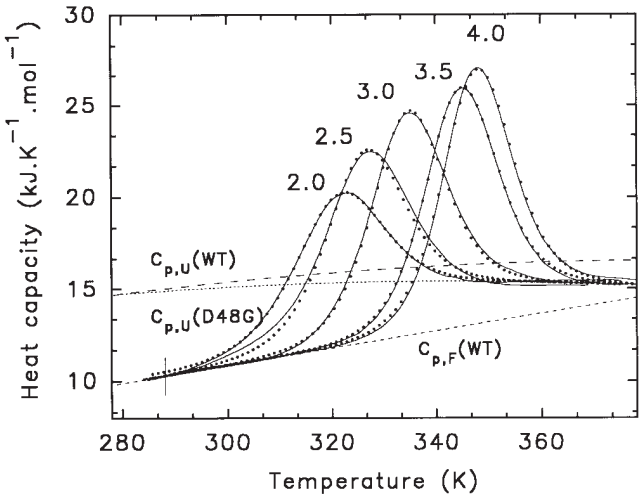

Fig. 2 Calorimetric traces at different pHs for the D48G protein. Temperature dependencies of the molar partial heat capacities of the SH3 D48G mutant at different acidic pHs (solid lines). Dots represent the best fit functions found from global curve-fitting to a two-state model[4]. As dashed lines we show the temperature functions of the heat capacity for the folded ($C_{p,F}$-WT) and unfolded states ($C_{p,U}$-WT) in the wild type protein and in the D48G mutant ($C_{p,U}$-D48G). The vertical bar at 288 K shows the scatter in the position of the curves on the heat capacity scale.

theories[14,15,19] in the new view of folding protein for two-state proteins are related to the conformational breadth of the transition state ensemble, and to the existence of obligatory steps in the folding reaction.

In this work we have addressed the question of how heterogeneous the transition state is, as well as the existence of obligatory steps in protein folding which do not necessarily favor the folding reaction. The protein we have chosen for this study is the α-spectrin SH3 domain (62 residues) which folds into an orthogonal β-sandwich containing three β-hairpins[20,21], and follows a two-state folding mechanism[4]. This protein has been used to assess the effect of altering the order of secondary structure elements (circular permutants)[22,18], as well as the importance of loop length on protein folding and stability[23].

To test the above question we have mutated D48G in the type II' β-turn of the SH3 distal loop, and introduced several other point mutations previously used to analyze the structure of the transition state in the wild-type protein into the D48G mutant (Fig. 1*a*). This mutation stabilizes the protein significantly through a local conformational change of the turn, and produces a 20-fold acceleration of the folding reaction without affecting the unfolding rate. Therefore, it is an ideal model to analyze the heterogeneity of the transition state ensemble.

Rationale behind the D48G mutation

X-ray[20] and NMR[21] analyses of the α-spectrin SH3 structure show that Asn 47 located at position *i+1* of a type II' β-turn (Richardson classification) in the distal loop (Fig. 1*a*) is in a forbidden region of the Ramachandran plot (ϕ = 43.4° and ψ = -90.1°). The sequence in this β-turn is Val 46-Asn 47-Asp 48-Arg 49, and the Asn residue does not make contacts with the rest of the protein. Protein engineering analysis[12] has shown that in the wild type protein the folding nucleus is partly located on a β-hairpin containing this β-turn[18] (Fig. 1*a*). On the other hand, we know that the folding rate of the wild type α-spectrin SH3 domain is slow compared with other all β-sheet proteins of the same size[24]. Therefore, it is possible that one of the factors limiting the folding rate is the formation of this β-turn, forcing Asn 47 to adopt forbidden or energetically very unfavorable dihedral angles. Structural analysis of several mutants at the turn position of a model β-hairpin peptide[25] has shown that the optimum sequence for a two residue β-turn in a β-hairpin is Asn-Gly at positions *i+1* and *i+2*. Thus, it should be possible to create a very favorable type I' β-turn with the sequence V46-N47-G48-R49 without disturbing the rest of the protein and, as a consequence, a barrier in the folding process of this protein could be removed.

Structure of the mutant protein

The crystal structure of the D48G α-spectrin SH3 mutant has

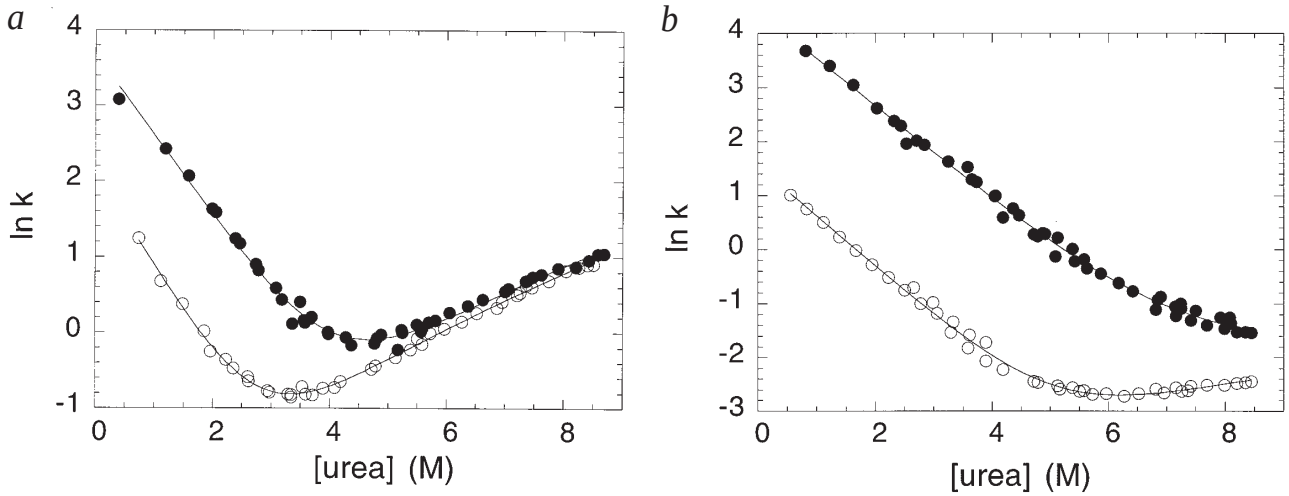

Fig. 3 Kinetic measurements of the unfolding and refolding reaction of α-spectrin SH3 domain. Urea concentration dependence of the natural logarithm of the rate constants for refolding and unfolding. Empty circles are wild type data and filled circles the D48G mutant ones: ***a***, pH 3.5. ***b***, pH 7.0. The solid lines represent the best fit of the whole data set to the equation (5) described in the Methods.

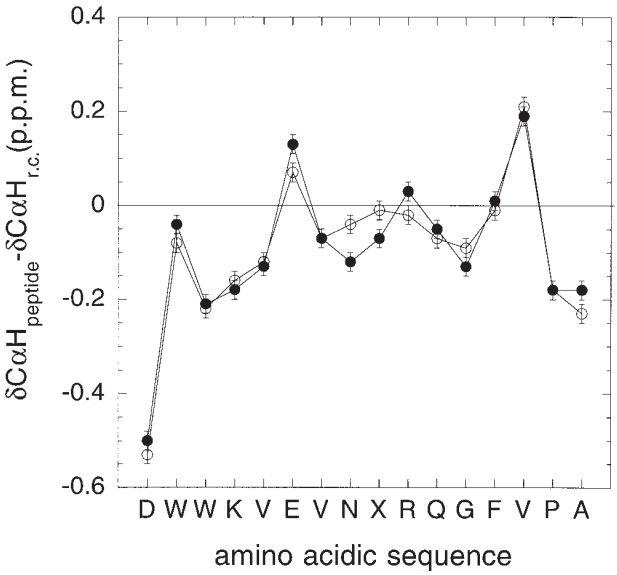

Fig. 4 Conformational shift plot of the CαH protons for the distal β-hairpin fragment. In this figure we show the differences between the chemical shifts for the CαH protons of a peptide including the whole sequence corresponding to the distal β-hairpin and the corresponding random coil values[57]. The X is an Asp in the wild type protein and a Gly in the D48G mutant. In the case of the Gly residues we show the average of the two protons. Empty circles are wild type data and filled circles the D48G mutant ones.

been solved at a resolution of 2.01 Å by molecular replacement using the wt α-spectrin SH3 structure (1SHG entry in the PDB; Table 1). The three-dimensional fold is virtually identical to the fold of the wild type α-spectrin SH3 domain, except in the region of the β-turn (Fig. 1*b*), and the two structures superimpose with a root-mean-square deviation (r.m.s.d.) of 0.47 Å for all Cα atoms. The conformation of the two-residue turn at the distal loop is not identical in the wild type and D48G proteins, differing mainly at the dihedral angles of residues 47 (WT, ϕ = 43.4° and ψ = -90.1°; D48G, ϕ = 20.7° and ψ = 48.4°) and 48 (WT, ϕ = 66.7 and ψ = 32.41° ; D48G, ϕ = -108.5 and ψ = -10.3°) (Fig. 1*b*). In both structures this turn is rather flexible, as shown by the high B-factors and, as expected, it is not directly involved in contacts with the rest of the protein.

Protein stability

Mutation of Asp 48 to Gly introduces more degrees of freedom in the polypeptide chain as well as allowing the turn to adopt a more relaxed conformation with no residues in the forbidden area of the Ramachandran plot. Table 2 shows the differences in Gibbs energy between the two proteins determined from calorimetry at different pH values, and Table 3 shows the Gibbs energy values obtained from analysis of the folding and unfolding kinetics at pH 3.5 and 7.0. Mutation of Asp 48 to Gly results in a significant stabilization of the protein (between 3–4 Kj mol^{-1}, depending on pH). Differential scanning calorimetry analysis (DSC) indicates that this change seems to be mainly of entropic origin, in good agreement with the crystal structure, which shows no new contacts. The heat capacity of the denatured state at pH values higher than 3.0 seems to be different in both proteins, being lower in the D48G mutant (Fig. 2; Table 2).

Kinetic analysis

The variation of the unfolding and refolding rate constants for the D48G and the wild type proteins with urea at pH 3.5 and 7.0 are shown in Fig. 3. Table 3 shows the extrapolated values to native conditions. From the kinetic data, the destabilization of the protein induced by the mutation ($\Delta\Delta G_{F\text{-}U}$), and its components in the refolding ($\Delta\Delta G_{‡\text{-}U}$) and unfolding semi-reactions ($\Delta\Delta G_{‡\text{-}F}$) can be calculated. The kinetic slopes $m_{‡\text{-}F}$ (related to the difference in solvent accessibility between the folded and transition states) are the same for both proteins, within the experimental error (± 0.02), in the unfolding reaction at pH 3.5. Also, all the destabilizing mutations we have made in the D48G protein have $m_{‡\text{-}F}$ values at pH 7.0 similar to those of wild type (data not shown). Based on these results, the $m_{‡\text{-}F}$ value of wild type at pH 7.0 was used to fit the D48G data, since under these conditions there is a large degree of uncertainty in the fitting of the mutant due to its high stability (Fig. 3*b*). However, the kinetic refolding slope ($m_{‡\text{-}U}$) for the D48G mutant (related to the difference in solvent accessibility between the denatured and transition states) is smaller than in the wild type protein at both pH 3.5 and 7.0, as well as in the different mutants (data not shown). This — together with the differences in the heat capacity of the denatured state at pH values higher than 3.0 — indicates a slight compaction of the denatured state in water, which is in agreement with the calorimetric analysis. The protein engineering analysis of the D48G mutation (see Methods) results in a $\phi_{‡\text{-}U}$ value of ~1 at both, pH 3.5 and 7.0, which implies that the β-turn is fully formed in the transition state of this protein.

NMR analysis of the distal loop fragment

The denatured ensemble of the D48G mutant is, on average, slightly more compact than in the wild type protein at pH values higher than 3.0. Based on this, it can be postulated that the β-hairpin containing the distal loop is stabilized upon mutation of Asp 48 to Gly, becoming more structured. To see if this is so, we have analyzed a peptide including residues 40–55 by nuclear magnetic resonance (NMR). We could not find any NOE evidence for the formation of a stable hairpin or a β-turn at the expected position (data not shown). However, line broadening and population fluctuations could mask any new NOEs resulting from an increase in hairpin population. An independent NMR parameter that is related to changes in structured populations is the conformational shifts of the CαH protons (δΔCαH). Comparison of the δΔCαH values between the wild type peptide[22] and the D48G mutant peptide showed that, apart from small changes around the substituted position 48, they are identical within the error of the experiment (Fig. 4). This, together with the presence of several aromatic residues (which produce major conformationally dependent ring current effects on the neighboring Cα chemical shifts), supports the idea that no major conformational changes result from the mutation. Thus, it seems that the compaction of the denatured ensemble cannot be explained solely by a significant increase of β-hairpin structure.

D48G mutant transition state

To determine if stabilization of the transition state by the D48G mutation changes its conformational ensemble, a series of mutations, previously analyzed in the wild type protein, and which act as reporters of the transition state ensemble structure, have been carried out[18]. Kinetic analysis of the different

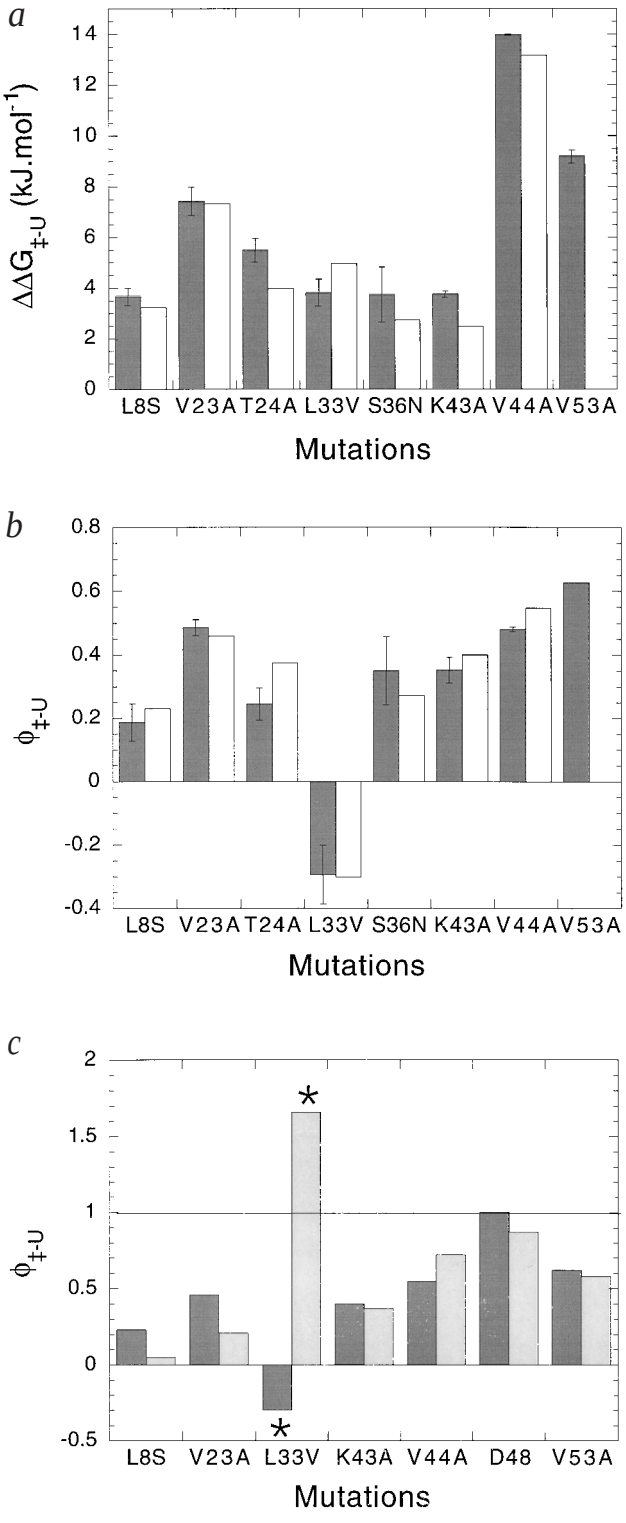

Fig. 5 Energetic analysis of the different mutations. **a**, Destabilization energy $\Delta\Delta G_{F\text{-}U}$ induced by each point mutation in the wild type (white bars) and D48G proteins (filled bars) at pH 7.0. The errors for the D48G mutants are shown. ***b***, $\phi_{\ddagger\text{-}U}$ values ($\Delta\Delta G_{\ddagger\text{-}U}/\Delta\Delta G_{F\text{-}U}$) obtained for wild type (white bars) and D48G mutants (filled bars) at pH 7.0. This ratio reflects the extent to which the deleted interaction is present in the transition state of the reference protein (wild type or D48G). Data on mutant V53A for wild type is missing because it could not be purified. ***c***, Comparison between the $\phi_{\ddagger\text{-}U}$ values for equivalent mutations in the α-spectrin (dark gray bars) and src SH3 mutants (gray bars)[38]. The equivalent positions in src SH3 are Leu 24 for Val 23, Ile 34 for Leu 33, Leu 44 for Lys 43, Ala 45 for Val 44, Ile 56 for Val 53 (the data shown for α-spectrin is that obtained in the D48G protein). In the case of Leu 8 there is no equivalent mutation although we can compare it with the results for Phe 10 in src, since both are probing the same region. Regarding Asp 48, there is no equivalent position in src, since the turn geometry is different, therefore we have used an average $\phi_{\ddagger\text{-}U}$ value for the three src SH3 mutants at the distal loop. *Residues showing non-native interactions (see text).

mutations in the D48G protein was done at pH 7.0. In all the cases it was possible to fit the data to a two state process, with unfolding and refolding slopes similar to those found in the same mutations in the wild type protein (the only difference being a smaller value on average for $m_{\ddagger\text{-}U}$; data not shown). In Fig. 5*a* we show the differences in Gibbs energy found for the different mutants in the D48G protein, as well as on the wild type protein. The reference for the D48G mutant series was the D48G protein. We observe that, within the experimental error, the same differences in Gibbs energy with respect to the reference protein were obtained for all mutations. This corroborates the X-ray analysis which shows no structural differences between the wild type and D48G proteins, except at positions 47 and 48, and also indicates that the slight compaction produced on the denatured state by the D48G mutation does not significantly alter the energetics of this state.

In Fig. 5*b* we plot the $\phi_{\ddagger\text{-}U}$ values for all the mutants with respect either to the wild type or to the D48G protein. We found that, within the experimental error, all $\phi_{\ddagger\text{-}U}$ values are identical and, therefore, that the stabilization of the protein through the D48G mutation does not change the transition state.

β-turn conformation and protein stability

The role of β-turns in protein folding and stability has long been controversial. Proteins can tolerate a large sequence variability in turn regions[26,27], with some significant exceptions[28]. However, while turn residues do not seem to dictate the protein fold, they can affect protein thermodynamic stability significantly[29–32] as well as folding kinetics[22,33,34]. It has been found that optimum sequences for β-turn formation significantly stabilize the protein and, in many cases, produce an acceleration of the folding reaction[32]. In the case of isolated β-hairpin structures in model peptides free of context effects, we have found that the sequence present at the central positions of a two-residue turn has a significant effect on the stability of the hairpin[25].

The effects observed in the α-spectrin SH3 domain upon introduction of the D48G mutation support all the above observations, and indicate that β-turns could play a critical role in protein stability and folding velocities, constituting a prime target in protein design.

Comparison to other two-state proteins

In previous work we analyzed the transition state of the wild type α-spectrin SH3 domain[18,35]. The general picture we obtained from the different mutations in the wild type protein (positions, 8, 14, 23, 24, 36, 43, 44 and 53) suggests that residues located on the distal hairpin, as well as on the second β-strand of the RT loop that interacts with it, are more structured in the transition state than other parts of the protein. However, none of the mutants we tested before (Fig. 1*a*) resulted in $\phi_{\ddagger\text{-}U}$ values of 0 or 1, but intermediate values (Fig. 5*b*). Similar results have been found for other two-state proteins like CI-2[17] (with the exception of Ala 16 that has a $\phi_{\ddagger\text{-}U}$ value of ~1.0) and the Arc repressor[36]. In general, it is found that in those proteins mutations affecting

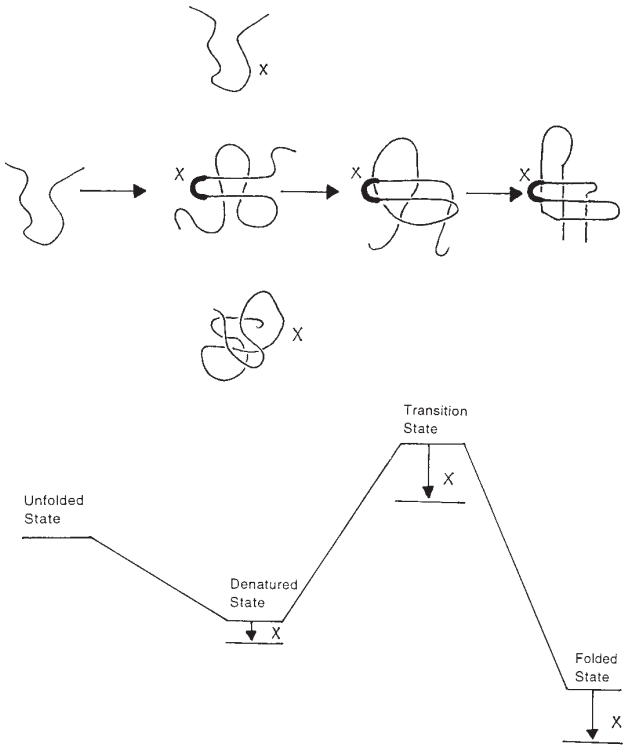

Fig. 6 Schematic diagram for the folding reaction of the SH3 protein. Unfolded state: the protein in strong denaturing conditions. Denatured state: the denatured protein under native conditions. Transition state: the highest energy point in the folding reaction. Folded state: the native conformation. The stabilizing point mutation at position 48 is shown as an X and the β-turn is shown as a bold curve. In the denatured state the hairpin may be folded in some of the conformations. Since the hairpin by itself is not folded in water, this means that only those compact conformations stabilizing the hairpin will be significantly represented. Stabilization of the turn will favor those conformations and produce, on average, a more compact denatured state. Folding will be initiated through a search of conformations until certain specific interactions, which act as a scaffold for subsequent contacts, are formed (folding nucleus). This implies formation of the distal hairpin in the α-spectrin SH3 and, consequently, full formation of the distal β-turn. Once this 'nucleus' is built, the protein passes over the transition state and then follows the downhill rapid cooperative formation of the folded structure.

residues in the hydrophobic core have higher $\phi_{\ddagger\text{-}U}$ values than those on the surface of the protein. This picture is consistent with the nucleation-condensation mechanism of protein folding[19,37]. Independently of the analysis performed by us on the α-spectrin SH3 domain, the group of Baker and co-workers have performed an extensive protein engineering analysis on the src SH3 domain[38]. There is a very good qualitative agreement between the results obtained for equivalent positions in both SH3 domains, especially at the putative folding nucleus of α-spectrin SH3 domain, although the sequence homology is only ~36% (Fig. 5*c*). Of particular interest is the fact that, in both proteins, residue 33 (α-spectrin numbering, position 34 in src) has $\phi_{\ddagger\text{-}U}$ values indicative of non-native interactions in the transition state, and that the β-turn region (distal loop) exhibits the highest $\phi_{\ddagger\text{-}U}$ values.

Obligatory steps in protein folding

The fact that in these two SH3 proteins the distal loop is the region that exhibits highest $\phi_{\ddagger\text{-}U}$ values is quite remarkable, since in all other small two-state proteins analyzed the regions with highest values are normally localized in the hydrophobic core. More strikingly, the residues at the distal loop are not conserved at all in the SH3 family[39]. This would indicate that some fully solvent exposed regions in the protein could be fully folded in the transition state, while the hydrophobic core or secondary structure elements may only be partly unfolded. However, we do not believe there is a contradiction between our results and those obtained in other systems. We have found that mutation of the turn region neither results in formation of the turn by itself in aqueous solution, nor does it produce an experimentally detectable significant enhancement of the β-hairpin population in the denatured state. This means that the turn *per se* cannot be formed in the transition state, in the absence of other stabilizing interactions. Its formation is an obligatory step resulting from the formation of the folding nucleus (see Fig. 6). The reason behind this is that its formation in the transition state is an obligatory step resulting from a topological constraint produced by the formation of the folding nucleus (the folding nucleus involves residues on both strands of the hairpin) Therefore, in protein folding we should distinguish between obligatory steps on the folding pathway, resulting from topological constraints that do not necessarily contribute to the formation of the folding nucleus but cannot be avoided by the protein, and the folding nucleus.

Homogeneity of the transition state

We can contemplate three possible scenarios for the transition state in the folding reaction of a protein. (i) The folding process could be seen as a parallel flow of an ensemble of chain molecules that follow multiple folding routes to reach the native state[14]. In this case, there is not a specific folding nucleus ('delocalized nucleus'), and any mutation that will stabilize or destabilize a large subset of those folding routes should shift the conformational distribution and result in a different transition state ensemble (Fig. 7*a*). (ii) The majority of the molecules pass through a single Gibbs energy barrier in which sufficient nonspecific tertiary interactions that offset the folding entropic cost are formed ('energetic nucleus'). Once this energetic nucleus is built, the protein passes over the transition state and then follows the rapid cooperative formation of the folded structure. Under these conditions, any mutation that stabilizes the folding nucleus will shift the transition state ensemble towards the denatured state (Fig. 7*b*). The opposite will happen with a destabilizing mutation. (iii) The folding nucleus is quite specific ('mechanic nucleus'), and requires the obligatory formation of certain interactions or local conformations (obligatory steps) to offset the folding entropic cost. In this case, part of the structure of the transition state will be quite impervious to energy changes (Fig. 7*c*).

The above scenarios cannot be discriminated by the presence of fractional $\phi_{\ddagger\text{-}U}$ values, but only by the behavior of these values when the protein either is stabilized or destabilized. Under the first and second scenarios, we expect that the protein engineering analysis of different mutations performed on a mutant protein with different stability will result in $\phi_{\ddagger\text{-}U}$ values different from those found on the wild type protein. In the first case, the changes in $\phi_{\ddagger\text{-}U}$ values could be random (that is, some will be higher and some lower), while in the second case, there will be an overall tendency for them to be lower if the transition state is stabilized, and *vice versa*. Under the third scenario, we should expect that the $\phi_{\ddagger\text{-}U}$ values of the residues corresponding to the folding nucleus will be the same in the wild type and in the mutant protein.

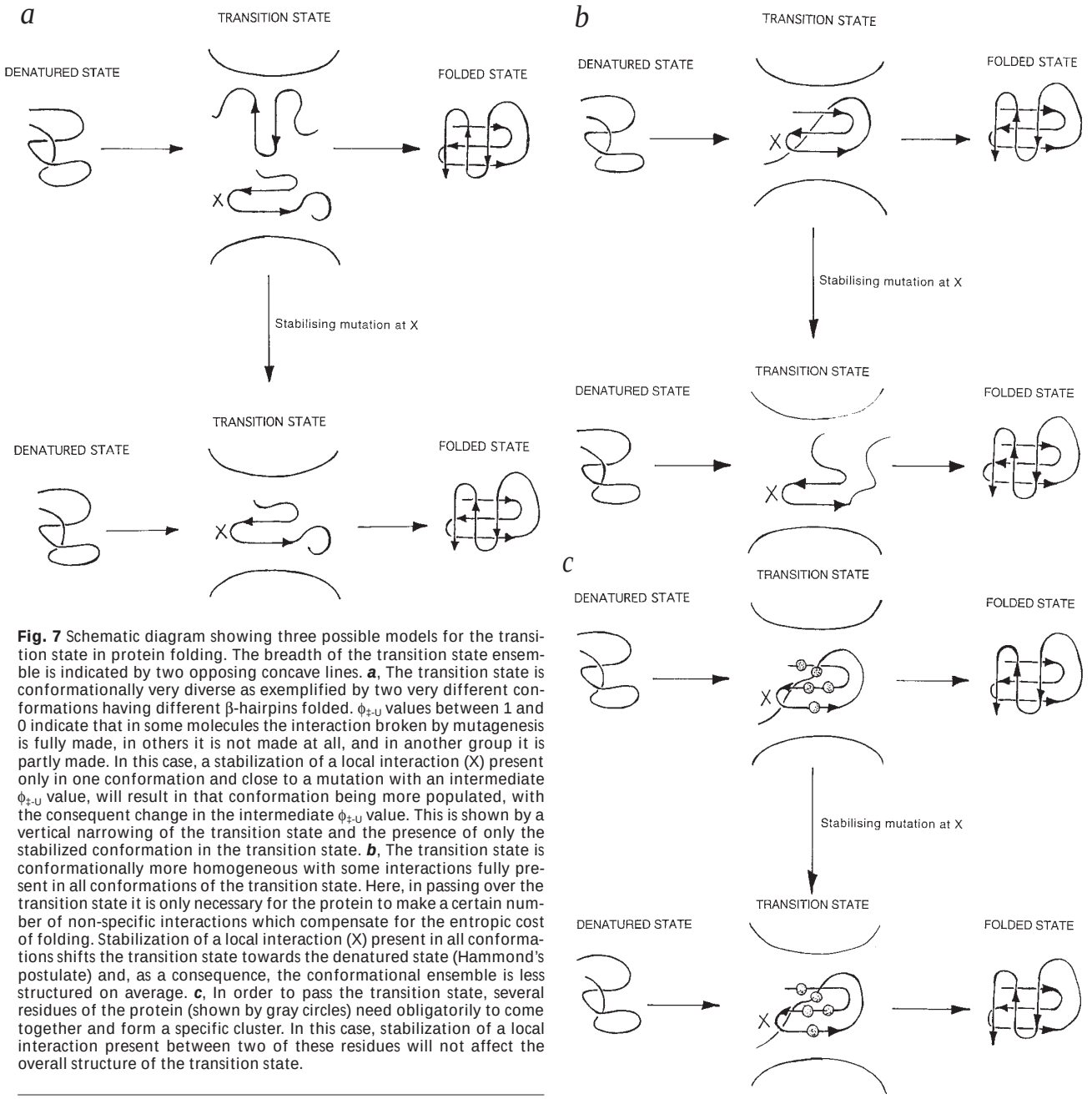

Fig. 7 Schematic diagram showing three possible models for the transition state in protein folding. The breadth of the transition state ensemble is indicated by two opposing concave lines. ***a***, The transition state is conformationally very diverse as exemplified by two very different conformations having different β-hairpins folded. $\phi_{\ddagger\text{-}U}$ values between 1 and 0 indicate that in some molecules the interaction broken by mutagenesis is fully made, in others it is not made at all, and in another group it is partly made. In this case, a stabilization of a local interaction (X) present only in one conformation and close to a mutation with an intermediate $\phi_{\ddagger\text{-}U}$ value, will result in that conformation being more populated, with the consequent change in the intermediate $\phi_{\ddagger\text{-}U}$ value. This is shown by a vertical narrowing of the transition state and the presence of only the stabilized conformation in the transition state. ***b***, The transition state is conformationally more homogeneous with some interactions fully present in all conformations of the transition state. Here, in passing over the transition state it is only necessary for the protein to make a certain number of non-specific interactions which compensate for the entropic cost of folding. Stabilization of a local interaction (X) present in all conformations shifts the transition state towards the denatured state (Hammond's postulate) and, as a consequence, the conformational ensemble is less structured on average. ***c***, In order to pass the transition state, several residues of the protein (shown by gray circles) need obligatorily to come together and form a specific cluster. In this case, stabilization of a local interaction present between two of these residues will not affect the overall structure of the transition state.

Within the experimental limitations, the conservation of the $\phi_{\ddagger\text{-}U}$ values for eight mutations that, overall, probe the entire structure of the D48G α-spectrin SH3 mutant, indicates that model (iii) is the most likely to apply for this domain. Moreover, the fact that the $\phi_{\ddagger\text{-}U}$ values for the putative folding nucleus in both α-spectrin and src SH3 domains[38] are similar when their sequences are not conserved also supports this model.

However, there is an apparent contradiction with the experimental results found for the protein engineering analysis of a circular permutant of this domain[18]. Comparison of the $\phi_{\ddagger\text{-}U}$ values for the same mutants analyzed here in the wild type protein, and a circular permutant with the N- and C-termini positioned between Asn 47 and Asp 48, showed the expected behavior described in model (i). Nevertheless, when this permutant was destabilized by elongating the newly created loop with Gly, we found that the $\phi_{\ddagger\text{-}U}$ value of a reporter point mutation at this region was not affected, as expected for model (iii).

Based on these results, we can conclude that passing through the transition state barrier in some proteins requires formation of a defined structure with little conformational variability in some regions, as postulated by Abkevich and coworkers[19]. In the presence of drastic mutations (for example, circular permutation of a protein[18]), alternative transition state ensembles scarcely populated can be revealed; but these new transition state ensembles could again have a defined structure with little conformational variability. Our results and those of Baker's group[38] do not support the idea that conserved residues in proteins are necessarily the ones that play a critical role in folding[40]. However, we cannot rule out that under a less restricted definition of residue conservation, the hypothesis proposed by Shakhnovich and coworkers[40] could hold.

Different folds and transition states

A conformationally restricted transition state does not necessarily need to be universal, and it probably occurs in the SH3 domain because of the rigidity imposed by the hydrogen-bond network required for the formation of β-sheet structures, as has been recently proposed by Perl and co-workers[24]. In fact, although these authors found a conservation of the rate of folding in the DspB family and used this as an argument for their hypothesis, this is not the case in the SH3 family[41]. For all α-helical proteins, or proteins containing α-helices, the transition state ensemble could be closer to models (i) or (ii) and, therefore, their transition states could be much more sensitive to the effect of simple point mutations. This seems to be the case for λ repressor where mutations shift the position of the transition state, as shown by the large changes in the refolding and unfolding slopes[42].

The existence of different folding scenarios for all α-helical proteins and other 'more complex' protein folds has been discussed by Wolynes and co-workers[15], who suggest that the presence of delocalized nuclei on the folding pathway may occur for small all-helical proteins, but it may not be so in more complex systems for two reasons: (i) the presence of geometric traps, and/or (ii) the large inhomogeneity of the ensemble, so that the transmission coefficient for folding greatly exceeds the entropic advantage of using the other states. More experiments need to be performed on these and other proteins to clarify to what extent the transition state is homogenous, and if there is any correlation between the fold type and the inhomogeneity of this state.

Methods

Mutagenesis and purification. The mutants, obtained by the polymerase chain reaction (PCR) method[43], were expressed and purified as described[4]. Protein concentration was determined using the method of Gill & Von Hippel[44] to obtain the extinction coefficient, 2.26 cm^{-1} mg^{-1} ml (the same value found for the WILD TYPE domain).

Crystallography. Crystals of the D48G mutant were obtained by the hanging drop method. Drops of 2 µl protein solution (8 mg ml^{-1}) were added to 4–8 µl of reservoir solution (1.1 M ammonium sulfate, 90 mM sodium citrate/citric acid, pH 6.0, 90 mM bis-Tris propane, 0.9 mM EDTA, 0.9 mM DTT, 0.9 mM sodium azide) at room temperature. Rectangular crystals with maximum dimensions 800 × 200 × 200 $µm^3$ appeared after 2–3 days.

Crystals were transferred into a solution that contained 90% [v/v] reservoir solution and 10% [v/v] glycerol. These crystals were then shock-frozen at 100 K within maximum of five minutes after transfer. All crystallographic data were obtained under cryo-cooling conditions using an Oxford CryoSystem cryo-stream instrument with in-house Cu-Kα X-ray generators. The X-ray data were recorded on a Small Mar imaging plate (radius = 90 mm) mounted on a Siemens/MacScience MX18 generator. Data were processed with the programs DENZO and SCALEPACK[45]. The structure was solved by molecular replacement and rigid-body refined with the AMORE program package[46] using the wild-type α-spectrin SH3 domain structure[20] as molecular template. The correct solution had an R-factor of 27.6% and a correlation coefficient of 0.85. The structure was refined by an iterative procedure using the graphics program O[47], the refinement package X-PLOR[48] and the ARP package[49]. Several programs of the CCP4 suite were used (SERC collaborative computing project number 4). The crystallographic statistics are summarized in Table 1.

Table 1 Crystallographic data statistics for the D48G mutant

Resolution (Å)	2.01
Space group	$P2_12_12_1$
Unit cell (Å)	33.25; 42.22; 49.87
Molecules per asymmetric unit	1
Number of observations	47,630
Number of unique refl.	4,758
Completeness (%)	96.5
Total R_{merge} (%)	4.4
Number water molecules	50
Final R-factor (%)	22.4
Final R_{free} (%)	30.5
R.m.s.d. in bond lengths (Å)	0.015
R.m.s.d. in bond angles (Å)	1.830
Average B-factor ($Å^2$)	35.29

^{1}H-NMR spectroscopy. NMR samples were prepared in $H_2O/^2H_2O$ 9:1 (v/v) 5 mM sodium phosphate. Minute amounts of HCl and NaOH were added to adjust the pH of the samples to 5.4, measured with an Ingold combination electrode (Wilmad) inside the NMR tube. Protein concentration varied around 1 mM. Sodium 3-trimethylsilyl (2,2,3,3-$^2H_4$) propionate (TSP) was used as an internal reference at 0.00 p.p.m. NMR experiments were performed at a temperature of 278 K on a Bruker DMX-500 or 600 pulse spectrometer, and the data were processed with the program UXNMR from Bruker. One-dimensional spectra were acquired with 32K data points which were zero filled to 64K data points before Fourier transformation. All the two-dimensional spectra were acquired in the phase sensitive mode using the time proportional phase incrementation (TPPI) technique. COSY, DQFCOSY and NOESY spectra were recorded using standard phase-cycling sequences[50–53] and accumulating 8–64 scans per increment. TOCSY spectra were acquired using the standard MLEV17 spinlock sequence[54] and 80 ms mixing time. The spectral width used was 6666.66 Hz and presaturation of the water signal was done during the relaxation delay

Table 2 Thermodynamic parameters extracted from DSC experiments

pH	Name	T_m[1] (K)	$\Delta C_{p,U}(T_m)$[1] (kJ K^{-1} mol^{-1})	$\Delta H_U(T_m)$[1] (kJ mol^{-1})	$\Delta S_U(298)$[1] (J K^{-1} mol^{-1})	$\Delta G_U(298)$[1] (kJ mol^{-1})
2.0	wild type[2]	307.0	3.7	93	190	2.3
	D48G	318.3	3.6	140	180	6.4
2.5	wild type[2]	320.0	3.4	139	175	6.9
	D48G	324.6	3.4	170	165	9.8
3.0	wild type[2]	331.0	3.0	174	160	11.6
	D48G	333.4	3.0	196	150	14.0
3.5	wild type[2]	336.0	2.9	188	155	13.9
	D48G	343.9	2.5	214	135	18.3
4.0	wild type[2]	339.0	2.8	197	150	15.6
	D48G	347.2	2.4	225	130	20.5

[1]The errors in experimental values of $\Delta H_U(T_m)$, $\Delta S_U(298)$ and $\Delta C_{p,U}(T_m)$ are ~8%, 20% for $\Delta G_U(298)$ and ~0.7 K for T_m.
[2]Data taken from Viguera *et al.*[4]

Table 3 Kinetic parameters for the wild type and D48G mutant proteins[1]

Protein	$m_{‡-F}$ (kJ mol^{-1} M^{-1})	$m_{‡-U}$ (kJ mol^{-1} M^{-1})	$k_{‡-F}$ (s^{-1})	$k_{‡-U}$ (s^{-1})	m_{F-U} kJ mol^{-1} M^{-1}	ΔG_{F-U} (kJ mol^{-1})
pH 3.5						
wild type	-1.38 ± 0.04	3.18 ± 0.08	0.060 ± 0.001	8.5 ± 0.4	4.56	12.14
D48G	-1.38 ± 0.04	2.85 ± 0.06	0.064 ± 0.007	39.8 ± 2.4	4.06	15.91
pH 7.0						
wild type	-1.05 ± 0.02	2.30 ± 0.05	0.006 ± 0.002	4.7 ± 0.3	3.35	16.32
D48G	-1.05[2]	2.10 ± 0.06	0.01 ± 0.002	75.9 ± 4.4	3.14	22.18

[1]The experimental conditions and analysis are described in the Methods section. The data shown here have been obtained from the fitting of the normalized data corresponding to two different experiments. The errors shown correspond to the fitting errors. Independent fitting of the two experiments produce differences which are in the same order than the errors shown here. $m_{‡-F}$ dependence of the natural logarithm of unfolding with urea. $m_{‡-U}$ dependence of the natural logarithm of refolding with urea. $k_{‡-F}$ unfolding rate constant in water. $k_{‡-U}$ refolding rate constant in water. m_{F-U} dependence of the natural logarithm of the equilibrium constant with urea, obtained from the kinetic parameters $m_{‡-F}$ and $m_{‡-U}$. ΔG_{F-U} Gibbs energy change of unfolding determined from the kinetic parameters.
[2]Value fixed in the fitting equation.

(1 s) and also during the mixing time (50–150 ms) of NOESY spectra. Size of acquisition data matrices was 2048 × 300–600 words in f_2 and f_1 respectively, and prior to Fourier transformation the 2D data matrix was multiplied by a phase-shifted square-sine bell window function in both dimensions and zero-filled to 2048 × 2048 words. NOE cross-peak intensities were evaluated by volume integration. The assignment of the ^{1}H-NMR spectra was done using the sequential assignment procedure[55].

Differential scanning calorimetry (DSC). Calorimetric experiments were performed with the computerized version of the DASM-4 microcalorimeter (Biopribor, Russia) with platinum cells of 0.47 ml volume at 1 and 2 K min^{-1}. Before filling into the cell, the samples were extensively dialyzed against buffers with the appropriate pH. Since the experiments were conducted between pH 2 and 4, buffers were either 50 mM glycine/HCl or 50 mM acetic acid/sodium acetate. The concentration of the protein in calorimetric experiments was between 2 and 6 mg ml^{-1}. The samples were routinely heated up to 383 K and then cooled slowly inside the calorimeter and reheated once again to check the reversibility of the unfolding. All the experiments recovered about 80% of their initial amplitude, depending on the exposure of the sample to high temperature. The calorimetric records were transformed into the temperature dependencies of the partial molar heat capacity and analyzed as described elsewhere[4] and below.

To fit the data we followed the two-state model, using a non-linear $C_{p,U}$ function as used in the wild type domain[4]. Moreover, we have performed a direct global fitting of all the curves to the model in order to get a unique and more reliable $\Delta C_{p,U}(T)$ function. The expression we obtained was:

$$\Delta C_{p,U}(T) = -2.39 + 0.076*T - 0.0001795*T^2 \text{ (kJ K}^{-1}\text{ mol}^{-1}\text{)} \quad (1)$$

The results of this global curve fitting procedure are shown in Fig. 2 and for comparison we include the C_p functions corresponding to the WILD TYPE domain[4]. The enthalpy values we obtained from the fitting (Table 2) follow (between the limits of error) the WILD TYPE ΔH_U (T_m) *versus* T_m correlation (data not shown).

Kinetic measurements. Folding and unfolding kinetics were followed in a Biologic Stopped-flow machine by fluorescence emission selected with a 305 nm cut-off filter upon excitation at 290 nm. The buffer used was 50 mM sodium phosphate pH 7.0 or 50 mM glycine/HCl pH 3.5. The cell chamber and the syringes were kept at 298 K. The fluorescence and far-UV kinetic traces have been shown to be identical[4]. Apparent kinetic constants were calculated by fitting the experimental traces to a mono-exponential transition by means of algorithms provided by Biologic Software. In the refolding reaction two main transitions were observed: a fast transition completed in less than 5 s and a slow one independent of urea with a kinetic constant of ~0.02 s^{-1}. The slow phase of refolding accounts for ~4 % of the total amplitude of fluorescence recovery and it is due to proline isomerization[4]. The first rapid phase in fluorescence change has been fitted to mono-exponentials where k, the rate constant at a given concentration of denaturant, is calculated. The *cis-trans* Pro isomerization slow refolding phase is not considered in this analysis.

Determination of the kinetic parameters. When studying the unfolding and refolding reactions of unstable α-spectrin SH3 mutants it has been found that the changes in the natural logarithm of the unfolding rate constant with urea are not linear and curve at high urea concentrations[18,35]. A similar phenomena has been recently described for barnase[56]. In both, barnase and wild type SH3 proteins, there is a discrepancy between the Gibbs energy determined by urea denaturation and the calorimetric data of ~5 kJ mol^{-1}. These discrepancies can be explained through the fact that the denaturant activity of urea (a_{den}) is not linear with urea concentration and follows equations 2 and 3:

$$\Delta G_{F-U} = \Delta G_{F-U,H2O} + \Delta n_b * R*T*\ln(1+K_b*a_{den}) \quad (2)$$

$$a_{den} = 0.9815*[\text{urea}] - 0.02978*[\text{urea}]^2 + 0.00308*[\text{urea}]^3 \quad (3)$$

where K_b and Δn_b are the average denaturant binding constant and an increment of the effective number of binding sites at protein unfolding respectively. This non-linear deviation is more evident at high urea concentrations. In many proteins the urea concentration at which half of the protein is denatured is around 4 M and the transition region is small, therefore the non-linearity cannot be detected but produces an under-estimation of the stability. In unstable mutants in which the transition region is around 1–2 M urea this non-linearity could be detected in the unfolding reaction. This is the case for the α-spectrin SH3 domain and barnase mutants.

In the α-spectrin SH3 domain, fitting of several of these unstable mutants has shown that the curvature of the unfolding data follows equation 4 (which also reproduces the data in barnase):

$$\ln k_{‡-F}([\text{urea}]) = \ln k_{‡-F} + m_{‡-F}*[\text{urea}] - 0.014 * [\text{urea}]^2 \quad (4)$$

Accordingly, the kinetic data were fitted to the equation:

$$\ln k([\text{urea}]) = \ln(k_{‡-U} * \exp(m_{‡-U} * [\text{urea}]) + k_{‡-F} * \exp(m_{‡-F} * [\text{urea}] - 0.014 * [\text{urea}]^2)) \quad (5)$$

where $k_{‡-U}$ and $k_{‡-F}$ are the refolding and unfolding rate constants in water, respectively. $m_{‡-U}$ and $m_{‡-F}$ are the slopes of ln k *versus* [urea] in the refolding and unfolding reactions, respectively. With these values, $\Delta\Delta G_{F-U}$ (the destabilization energy induced by the mutation) and $\Delta\Delta G_{‡-U}$ and $\Delta\Delta G_{‡-F}$ (its components in the refolding and unfolding semi-reactions) can be calculated:

$$\Delta\Delta G_{F-U} = (\Delta G_{F-U})_{ref} - (\Delta G_{F-U})_{mut} = \Delta\Delta G_{‡-U} - \Delta\Delta G_{‡-F} \quad (6)$$

$$\Delta\Delta G_{‡-U} = -R*T*\ln(k_{‡-U,ref}/k_{‡-U,mut)}\ \Delta\Delta G_{‡-F} = -R*T*\ln(k_{‡-F,ref}/k_{‡-F,mut}) \quad (7)$$

where 'ref' refers to the D48G mutant and 'mut' to each one of the eight mutations introduced into the former. Calculation of the Gibbs energy of unfolding, using a non-linear term in the unfolding reaction, produces a good agreement with the calorimetric data (Tables 2, 3), as it happened with barnase[56]. The ratio between the refolding component and the destabilization energy $\Delta\Delta G_{\ddagger\text{-}U}/\Delta\Delta G_{F\text{-}U}$ is the so called $\phi_{\ddagger\text{-}U}$ value, that provides some information about the extent of formation of a particular interaction in the transition state[12].

Coordinates. X-ray coordinates are being deposited at the Brookhaven Protein Data Bank (accession number 1bk2).

Acknowledgments

We thank I. Angrand for help with mutagenesis and molecular biology, G. Wallon and C. Vega for invaluable help with crystallographic techniques, and F. J. Blanco and M. Ramirez-Alvarado in NMR processing. We are also grateful to P. L. Mateo for the generous offer of calorimetric techniques. We are grateful to D. Baker for providing us with a copy of his manuscript regarding the analysis of the src SH3 domain prior to publication, as well as allowing us to discuss their unpublished results. J.C.M. is supported by a TMR fellowship from the EU. M.T.P. is supported by an EU biotechnology grant.

Received 10 April, 1998; accepted 25 June, 1998.

1. Jackson, S.E. & Fersht, A.R. Folding of chymotrypsin inhibitor 2. 1. Evidence for a two-state transition. *Biochemistry* **30**, 10428–10435 (1991).
2. Alexander, P., Orban, J. & Bryan, P. Kinetic analysis of folding and unfolding of the 56 amino acid IgG-binding domain of Streptococcal protein G. *Biochemistry* **31**, 7243–7248 (1992).
3. Sosnick, T.R., Mayne, L., Hiller, R. & Englander, S.W. The barriers in protein folding. *Nature Struct. Biol.* **1**, 149–156 (1992).
4. Viguera, A.R., Martinez, J.C., Filimonov, V.V., Mateo, P.L. & Serrano, L. Thermodynamic and kinetic analysis of the SH3 domain of spectrin shows a two-state folding transition. *Biochemistry* **33**, 2142–2150 (1994).
5. Schindler, T., Herrler, M., Marahiel, M.A. & Schmid, F.X. Extremely rapid protein folding in the absence of intermediates. *Nature Struct. Biol.* **2**, 663–673 (1995).
6. Huang, G.S. & Oas, T.G. Submillisecond folding of monomeric λ repressor. *Proc. Natl. Acad. Sci. USA* **92**, 6878–6882 (1995).
7. Villegas, V. *et al*. Evidence for a two-state transition in the folding process of the activation domain of human procarboxypeptidase A2. *Biochemistry* **34**, 15105–15110 (1995).
8. Kragelund, B.B., Robinson, C.V., Knudesn, J., Dobson, C.M. & Poulsen, F.M. Fast and one-step folding of closely and distantly related homologous proteins of a four-helix bundle family. *J. Mol. Biol.* **256**, 187–200 (1995).
9. Kuhlman, B., Boice, J.A., Fairman, R. & Raleigh, D.P. Structure and stability of the N-terminal domain of the ribosomal protein L9: evidence for rapid two-state folding. *Biochemistry* **37**, 1025–1032 (1998).
10. Plaxco, K.W. *et al*. The folding kinetics and thermodynamics of the Fyn-SH3 domain. *Biochemistry* **37**, 2529–2537 (1998).
11. Plaxco, K.W., Spitzfaden, C., Campbell, I.D. & Dobson, C.M. Rapid refolding of a proline-rich all beta-sheet fibronectin type III module. *Proc. Natl. Acad. Sci. USA* **93**, 10703–10706 (1996).
12. Fersht, A .R. Characterizing transition states in protein folding: an essential step in the puzzle. *Curr. Opin. Struct. Biol.* **5**, 79–84 (1995).
13. Munoz, V. & Serrano, L. Local vs non-local interactions in protein folding and stability. An experimentalist point of view. *Folding & Design* **1**, R71–R77. (1996).
14. Dill, K.A. & Sun Chan, H. From levinthal to pathways to funnels. *Nature Struct. Biol.* **4**, 10–19 (1998).
15. Onuchic, J.N., Socci, N.D., Luthey-Schulten, Z. & Wolynes, P.G. Protein folding funnels: the nature of the transition state ensemble. *Folding & Design* **1**, 441–450 (1996).
16. Lopez-Hernandez, E. & Serrano, L. Structure of the transition state for folding of the 129aa protein, CheY, resembles that of a smaller protein, CI-2. *Folding & Design* **1**, 43–55 (1996).
17. Itzhaki, L.S., Otzen, D.E. & Fersht, A.R. The structure of the transition state for folding of chymotrypsin inhibitor 2 analysed by protein engineering methods: Evidence for a nucleation-condensation mechanism for protein folding. *J. Mol. Biol.* **254**, 260–288 (1995).
18. Viguera, A.R. Wilmanns, M. & Serrano, L. Different folding transition states could result in the some native structure. *Nature Struct. Biol.* **3**, 874–880 (1996).
19. Abkevich, V.I., Gutin, A.M. & and Shakhnovich, E.I.. Specific nucleus as the transition state for protein folding: evidence from the lattice model. *Biochemistry* **33**, 10026–10036 (1994)
20. Musacchio, A., M. E. M. Noble, M. E. M, Pautit, R. Wierenga, R. & Saraste, M. Crystal structure of a src-homology 3 (SH3) domain. *Nature* **359**, 851–855 (1992).
21. Blanco, F.J., Ortiz, A.R. & Serrano, L. ^{1}H and ^{15}N-NMR assignment and solution structure of the SH3 domain of spectrin. Comparison with the crystal structure. *J. Biomol. NMR.* **9**, 347–357 (1997).
22. Viguera, A.R., Blanco, F.J. & Serrano, L. The order of secondary structure elements does not determine the structure of a protein but does affect its folding kinetics. *J. Mol. Biol.* **247**, 670–681 (1995).
23. Viguera, A.R. & Serrano, L. Loop length, intramolecular diffusion and protein folding. *Nature Struct. Biol.* **4**, 939–946 (1997).
24. Perl, D. *et al*. Conservation of rapid two-state folding in mesophilic, thermophilic and hyperthermophilic cold shock proteins. *Nature Struct. Biol.* **5**, 229–235 (1998).
25. Ramirez-Alvarado, M., Blanco, F.J., Niemann, H. & Serrano, L. Role of β-turns residues in ß-hairpin formation and stability in designed peptides. *J. Mol. Biol.* **273**, 898–912 (1997).
26. Brunet, A.P. *et al*. The role of turns in the structure of an α-helical protein. *Nature* **363**, 355–358 (1993).
27. Castagnoli, L., Vetriani, C. & Cesareni, C. Linking an easily detectable phenotype to the folding of a common structural motif. Selection of rare mutations that prevent the folding of Rop. *J. Mol. Biol.* **234**, 378–387 (1994).
28. Ybe, J.A. & Hecht, M.H. Sequence replacements in the central β-turn of plastocyanin. *Prot. Sci.* **5**, 814–824 (1996).
29. Hynes, T.R., Hodel, A. & Fox, R.O. Engineering alternative β-turn types in Staphylococcal nuclease. *Biochemistry* **33**, 5021–5030 (1994).
30. Predki, P.F., Agrawal, V., Brunger, A.T. & Regan, L. Amino acid substitutions in a surface turn modulate protein stability. *Nature Struct. Biol.* **3**, 54–58 (1996).
31. Zhou, H.X., Hoess, R.H. & deGrado, W.F. In vitro evolution of thermodynamically stable turns. *Nature Struct. Biol.* **3**, 446–451 (1996).
32. Ohage, E.C., Grami, W., Walter, M.M., Steinbacher, S. & Steipe, B. ß-turn propensities as paradigms for the analysis of structural motifs to engineer protein stability. *Prot. Sci.* **6**, 233–241 (1997).
33. Kim, K., Ramanathan, R. & Frieden, C. Intestinal fatty acid binding protein: a specific residue in one turn appears to stabilize the native structure and be responsible for slow folding. *Prot. Sci.* **6**, 364–372 (1997).
34. Gu H, Kim D, Baker D. Contrasting roles for symmetrically disposed beta-turns in the folding of a small protein. *J. Mol. Biol.* **274**, 588–596 (1997).
35. Prieto, J., Wilmanns, M., Jimenez, M.A., Rico, M. & Serrano, L. Non-native interactions in protein folding and stability: Introducing a helical tendency in the all β-sheet α-spectrin SH3 domain. *J. Mol. Biol.* **268**, 760–778 (1997).
36. Milla, M.E., Brown, B.M., Waldburger, C.D. & Sauer, R.T. P22 Arc repressor: transition state properties inferred from mutational effects on the rates of protein unfolding and refolding. *Biochemistry* **34**, 13914–13919 (1995).
37. Fersht, A.R., Itzhaki, L.S., elMasry, N., Matthews, J.M. & Otzen, D.E. . Single versus parallel pathways of protein folding and fractional formation of structure in the transition state. *Proc. Natl. Acad. Sci. USA* **91**, 10426–10429 (1994).
38. Grantcharova, V.P., Riddle, D.S., Santiago, J.V. & Baker, D. Important role of hydrogen bonds in the structurally polarized transition sate for folding of the src SH3 domain. *Nature Struct. Biol.* **5**, 714–720 (1998).
39. Musacchio, A., Wilmanns, M. & Saraste, M. Structure and function of the SH3 domains. *Progr. Biophys. Molec. Biol.* **61**, 283–297 (1994).
40. Shakhnovich, E., Abkevich, V. & Ptitsyn, O. Conserved residues and the mechanism of protein folding. *Nature* **379**, 96–98 (1996).
41. Plaxco, K.W. *et al*. The folding kinetics and thermodynamics of the Fyn-SH3 domain. *Biochemistry* **37**, 2529–2537 (1998).
42. Burton, R.E., Huang, G.S., Daugherty, M.A., Calderone, T.F. & Oas, G.T. The energy landscape of a fast-folding protein mapped by Ala-Gly protein. *Nature Struct. Biol.* **4**, 305–310 (1998).
43. Kunkel, T.A. Rapid and efficient site-directed mutagenesis without phenotypic selection. *Proc. Natl. Acad. Sci. USA* **82**, 488–492 (1985).
44. Gill S.C. & von Hippel. P.H. Calculation of protein extinction coefficients from amino acid sequence data. *Anal. Biochem.* **182**, 319–326 (1989).
45. Otwinowski, Z. & Minor, W. The HKL program suite. Unpublished programs.
46. Navaza, J. AMORE : An automated package for molecular replacement. *Acta Crystallogr.* A**50**, 157–163 (1994).
47. Jones, T.A., Zou, J.-Y., Cowan, S.W. & Kjeldgaard, M. Improved methods for building protein models in electron density maps and the location of errors in these models. *Acta Crystallogr.* A**47**, 110–119 (1991).
48. Brunger, A.T., Kuriyan, J. & Karplus, M. Crystallographic R factor refinement by molecular dynamics. *Science* **235**, 458–460 (1987).
49. Lamzin, V.S. & Wilson, K.S. Automated refinement of protein models. *Acta Crystallogr.* A**49**, 129–147 (1993).
50. Marion, D. & Wüthrich, K. Application of phase sensitive two-dimensional correlated spectroscopy (COSY) for measurement of proton-proton spin-spin coupling constants. *Biochem. Biophys. Res. Comm.* **113**, 967–974 (1983).
51. Aue, W.P., Bartholdi, E. & Ernst, R.R. Two dimensional spectroscopy. Application to nuclear magnetic resonance. *J. Chem. Phys.* **64**, 2229–2246 (1976).
52. Piantini, U., Sørensen, O. W., Ernst, R. R. Multiple quantum filters for elucidating NMR coupling networks. *J. Amer. Chem. Soc.* **104**, 6800–6801 (1982).
53. Kumar, A., Ernst, R.R. & Wüthrich, K. A two-dimensional nuclear Overhauser enhancement (2D NOE) experiment for the elucidation of complete proton-proton cross-relaxation networks in biological macromolecules. *Biochem. Biophys. Res. Comm.* **95**, 1–6 (1980)
54. Bax, A., & Davis, D. G. MLEV-17 based two-dimensional homonuclear magnetization transfer spectroscopy. *J. Magn. Reson.* **65**, 355–360. (1985).
55. Wüthrich, K. In *NMR of proteins and nucleic acids*. (John Wiley & sons, New York; 1986).
56. Johnson, C.M. & Fersht, A.R. Protein stability as a function of denaturant concentration: The thermal stability of barnase in the presence of urea. *Biochemistry* **34**, 6795–6804 (1995).
57. Merutka, G., Dyson, H.J. & Wright, P.E. Random coil ^{1}H chemical shifts obtained as a function of temperature and trifluoroethanol concentration for the peptide series GGXGG. *J. Biomol. NMR* **5**, 14–24 (1995).